



ÉCOLE POLYTECHNIQUE  
FÉDÉRALE DE LAUSANNE

## EXPERIMENTAL PHYSICS

### P8 - Nuclear Physics

# Study of Cobalt 57 decay with NaI and germanium detectors

School of Basic Sciences  
Physics

**Luc Testa and Justin Villard**

March 28, 2014

---

#### Abstract

This report is focused on decay processes and interaction between particles and matter. Firstly, we will find the approach of the statistic involved in nuclear phenomena and the analysis of the attenuation of radiation in matter. Then, measurements of some decay spectrums with two different kinds of detectors, a scintillation detector (NaI) and a semiconductor detector (Ge) are exposed. Finally, we present the determination of a  $^{57}\text{Co}$  source's activity and the period of the 14.4 keV level of  $^{57}\text{Fe}$ .

---

Group N°: 22

Manipulation N°: P8 Exp. 10

Assistant: Ilya Komarov

# 1 Introduction

Nuclear physics is the science that study the properties of atomic nucleus and its behaviour with other particules situated close to them. Nuclear physics is crucial to understand the structure of matter as well as nuclear reactions observed. One may find its applications for example in energy production and medical treatments. More precisely, this large domain contains the study of radioactive decays which describes the emission of particles and loss of energy of an unstable atom's nucleus.

This experiment will be focused on decay processes and interaction between particles and matter. After becoming familiar with the experimental devices by calculating a spectrometry chain, we will study a part of the statistic involved in nuclear phenomena. Then, we will analyze the attenuation of radiation in matter and measure some decay spectra with two different kinds of detectors, a scintillation detector and a semiconductor detector. Finally we will determine the activity of a  $^{57}\text{Co}$  source and the period of the 14.4 keV level of  $^{57}\text{Fe}$ .

## 2 Theoretical background

### 2.1 Nuclear reactions

It exists two main nuclear types of observable radiations. First is due to reactions that change the nature of nucleus and the other is simply the fact that atoms could evacuate some extra energy. The radiations coming from the nucleus can be presented in three forms:

- ▷  $\alpha$ , helium nucleus
- ▷  $\beta$ , electrons or positrons
- ▷  $\gamma$ , energetic photons

$\alpha$  radiation is related to the strong interaction,  $\beta$  the weak force and  $\gamma$  comes from the reorganisation of the nucleus structure. More details are mentionned in [1], chapter 1.

### 2.2 Photons interactions with matter

When photons hit matter, we can observe four main effects. Firstly, it appears that a photon can be absorbed by an atomic electron if this electron aquires sufficient energy to be ejected from its atom. This is called the photoelectric effect. If  $E_\gamma$  is the energy of the incident photon, and  $L_e$  the bonding energy of the electron, then we have the energy of the extracted electron

$$E_e = E_\gamma - L_e \quad (1)$$

Then, it could happen than photons are elasticly diffused by an electron af the matter. This is called the Compton effect. By using the energy and impulsion conservation, one may determine the energy won by the electron in function of the energy of the incident photon, with  $\theta$  the angle between incidence and final photon's directions.

$$E_e = \frac{E_\gamma}{1 + \frac{m_e c^2}{E_\gamma (1 - \cos \theta)}} \quad (2)$$

The maximum of energy of the scattered photon is so given by

$$E_{\gamma'}(max) = E_\gamma - E_\gamma(min) = \frac{E_\gamma}{1 + \frac{m_e c^2}{2E_\gamma}} \quad (3)$$

One particular case of this effect is back scattering, case when the incident photon is emitted to the rear as  $\gamma'$ . Thus we have

$$E_\gamma = E_{\gamma'} + E_e \quad (4)$$

and the energy of the scattered photon is given by

$$E_{\gamma'} = \frac{E_{\gamma}}{1 + \frac{2E_{\gamma}}{m_e c^2}} \quad (5)$$

We also find the pair production which is an effect that appears when the energy of the photon is higher than  $2m_e c^2$  (1.02 MeV). In this case, the photon can materialize itself in an electron-positron pair. Then the positron recombines itself with an electron of matter and two new photons  $2\gamma$  are emitted with an energy of 0.511 keV. This effect is really important in particles detection as with a semiconductor detector.

Finally, it appears that electrons can move and change the electronic structure in the atom when photons hit them. This is due to the jump of electrons between the electron shells. When this process delivers energy, we have a gamma emission such that

$$E_{\gamma} = h\nu_{i \rightarrow j} = E_j - E_i \quad (6)$$

with  $E_k$  the energy's level of the shell  $k=L, M, N$ , etc.

## 2.3 Particles detection, scintillation and semiconductor

There are a lot of particle detectors, depending of the kind particle that one wants to study. If it is a charged one, the principle is quite simple. Each positive or negative particle leave a trace such as ionisation or excitation of atoms close to them, because of their interaction with the matter. A detector is an instrument which will reveal this trace. The most common ones are electronic, they deliver an electric signal which can be analysed by computers, but there also are some "visual" detectors such as the Wilson room and bubbles rooms.

In the case of photons, we use the fact that the photon interacts with matter, which generally leads to a Compton effect, photoelectric effect or eventually pair creation. These processes free a positive or negative particle which can be detected by a classical detector.

In this manipulation, we will have to study the decay of an element, thus we will deal with photons  $\gamma$  of energy smaller than 10 MeV. We will use two different detectors: a scintillation counter and a semiconductor detector.

### 2.3.1 Scintillation counter

A scintillation counter is divided in two parts. The scintillator and the photomultiplier. The first one will emit an scintillation photon which be transformed in an electron and multiplied in the PM. This results in an electric signal which can be analysed by a computer.

When a charged particle goes into the detector, it automatically interacts with the matter. This leads to excitation and ionisation of the electrons in the detector. When they come back in their fundamental state, they emit a scintillation photon of energy proportional to the excitation level.

These photons are projected on the photocathode (*c.f. figure ??*). Thus, some electrons will be ejected through the PM by photoelectric effect. These electrons will be accelerated on dynodes and create more and more electron by secondary emission. This will amplify the incoming signal and lead to an electric signal which goes to the computer.

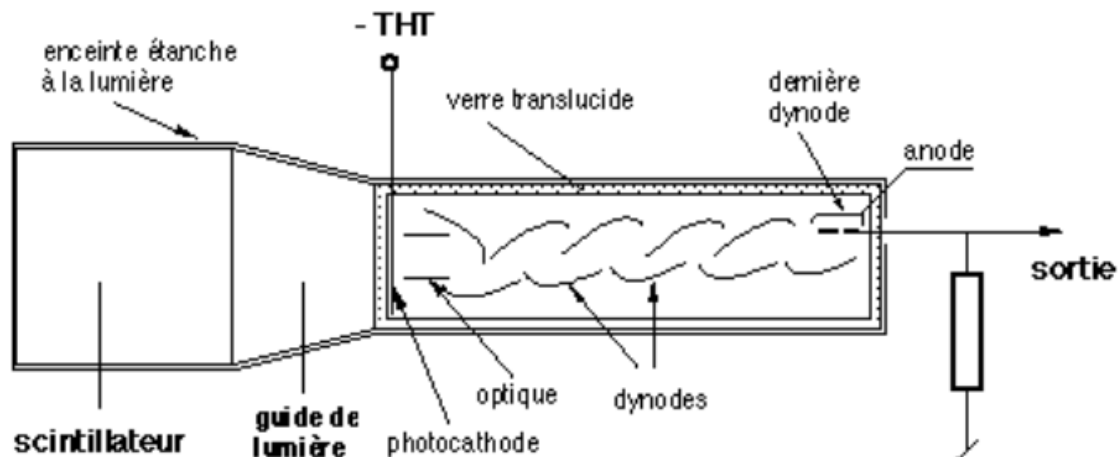


Figure 1: *Scintillation counter. Source:[1]*

### 2.3.2 Semiconductor detector

A semiconductor can be schematized like the following figure. There are two bands: the valence band and the conduction band. In general, the valence band is so full that the electron can nearly move. If they acquire a big enough kinetic energy  $E_e \geq \Delta E$ , they can "cross" the energy gap and join the conduction band where they are free to move.

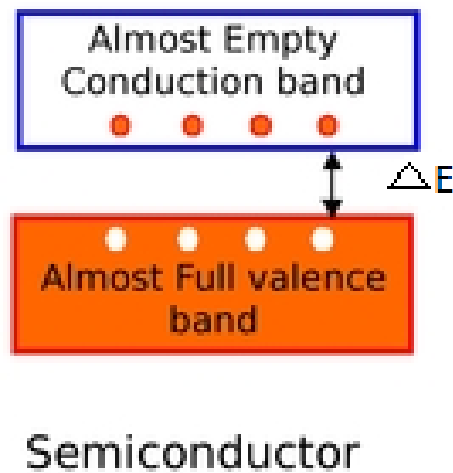


Figure 2: *Semiconductor. Schematization of the bands. Source: Wikipedia*

In a semiconductor detector, the incoming particle loses some energy to the matter. This results in the creation of electron-hole pairs. If we apply a tension in the detector, this will make all the free electrons move and lead in an observable current. This current is directly proportional to the energy of the electrons, and then to the energy of the incident particle. We thus get the spectra of the decay of our element.

Since this detector does not imply an avalanche of reactions, the resolution of a semiconductor detector is much higher than a scintillation counter.

### 2.3.3 $\gamma$ interactions with scintillation detector

With the use of lead collimation around the analyzed source and in the case of incident photons with energy  $E_\gamma$  smaller than 1.022 MeV ( $2m_e c^2$ ), the possible interactions in the scintillator (NaI) are the following as described in the figure below.

1-2. Photoelectric effect in the scintillator. When photon hits the NaI crystal, an electron results with a X radiation that comes from the reorganisation in the electronic structure. In general, the X is reabsorbed by the crystal and the peak in the spectrum corresponds to  $E_\gamma$ . Another case appears when  $E_\gamma$  is close to the energy of the K level jump. In this case, the X can escape and the energy detected corresponds to  $E_\gamma - E_X$ .

3-4. Compton effect without and with reabsorption of the  $\gamma'$  scattered.

5. Photoelectric effect in the lead collimation, followed by the absorption of the X in the NaI.

We also can find the situation in which the photon is reflected on the photomultiplier and scattered, the special Compton effect, back scattering.

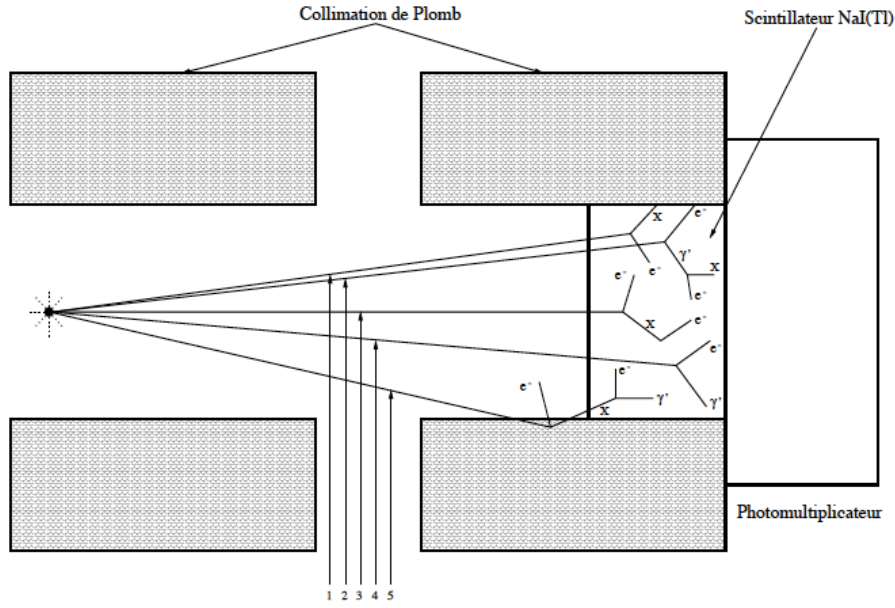


Figure 3: Possible interactions of photons in scintillator

## 2.4 Spectrometry chain with a scintillation detector

Our spectrometry chain is composed by a scintillation detector (with scintillating NaI crystal), followed by a photomultiplier (PM) and an emitter-follower (ES). Then we catch the signal with an amplifier, a discriminator and a multichannel analyzer. All specifications about these experimental devices can be found in the general notice [1], chapter 3, so that we will not repeat them here.

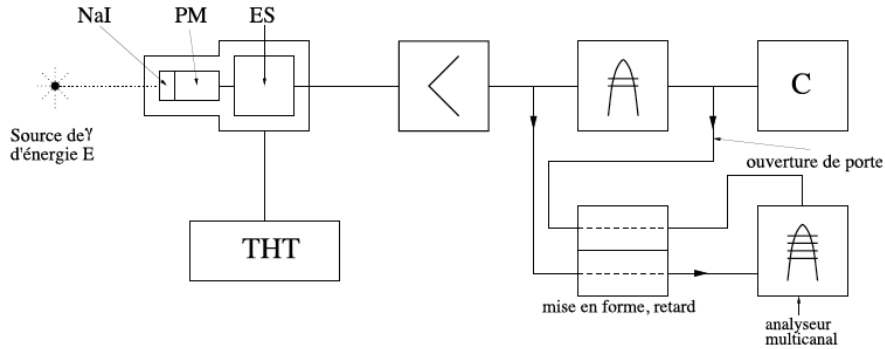


Figure 4: Spectrometry chain, experimental devices

Pulses (voltage) at the output of an apparatus in the chain must be adapted to the input of the next apparatus. Thus, the amplitude of the delivered pulse by the photomultiplier must be around 0.2 V. According to the notice [2] and section 2.5 of [1], one may determine the gain of the photomultiplier to obtain such a voltage at its output:

$$G = \frac{V \cdot h\nu \cdot C}{a(k) \cdot E \cdot \eta \cdot f \cdot \varepsilon \cdot e} \approx 1.8 \cdot 10^4 \quad (7)$$

where all parameters are known or can be found in manuals in lab and notices.  $V = 0.2V$  is the wanted voltage.  $h\nu = 3eV$  is the energy of a photon emitted by the scintillated crystal,  $C = 100pF$  is the capacity of the photomultiplier,  $E \simeq 1.4MeV$  is the highest value of photon energy that we will have (from  $\gamma_2$ ,  $^{60}Co$ ),  $\eta = 13\%$  is the scintillation efficiency,  $f = 50\%$  the ratio of scintillated photons at the photocathod (PM2202B),  $\varepsilon = 23\%$  the quantum efficiency of the photocathod and  $e = 1.602 \cdot 10^{19}C$  the elementary charge. We also have  $k = RC/\tau = 39\mu s/0.23\mu s = 169.57 \approx \infty$  so that  $a(k) = V/V_\infty = (1 - e^{-t/\tau}) \approx 1\forall t$ .

We then have to find the high voltage value of the photomultiplier to have this gain. In practice, we look at this voltage by having a 0.2V output on an oscilloscope. We finally apply a voltage of 800V.

The discriminator (or range analyzer) gives us two outputs, an analogic or a logic signal. The logic one can thus be used to open the window of the multichannel analyzer who receives the analogic signal. This method allows us to observe (on computer) directly the discrimination threshold and the window covered by the analyzer (coincidence method). Or, by observing these two signals on an oscilloscope, it may appear that they are shifted, with the logic one in advance. In this case, one must use a retarder to delay the analogic signal to ensure the same phase between the signals.

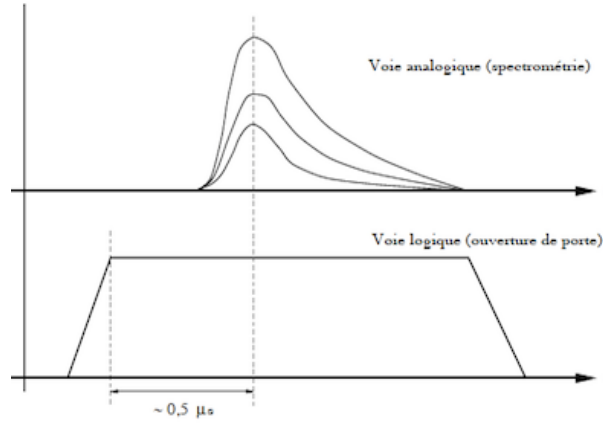


Figure 5: *Logic and analogic signals, coincidence method*

## 2.5 Statistical nature of nuclear phenomena

The goal of this section is to show that the statistical nature of the decay follows a Poisson distribution given by

$$f(k; \lambda) = \Pr(X = k) = \frac{\lambda^k e^{-\lambda}}{k!},$$

In order to do this, one will do several measures of the number of detection counted by the scintillator in a give time  $\Delta t$ . We will focus on a low mean value experiment and a high mean value experiment because we want to show that the last one tends to a Gaussian distribution, but if we prove that the distribution follows a Poisson distribution, it must follow a Gaussian for a high number of events. This is why we will only focus on the low mean value distribution.

### 2.5.1 Low mean value

We placed the sample of  $^{137}\text{Cs}$  at a given distance and led the experiment 256 times, with  $\Delta t = 12 \pm 1 \text{ ns}$ . We are then able to determinate some experimental and theoretical parameters such that

- The mean value  $\bar{N} = \frac{\sum_{i=1}^{256} N_i}{256}$
- The standard deviation  $\sigma_{\bar{N}} = \sqrt{\frac{1}{256} \sum_{i=1}^{256} (N_i - \bar{N})^2}$
- The theoretical Poisson standard deviation given by  $\sigma_{N,th} = \sqrt{\bar{N}}$

These three parameters are reported in the table below. It appears that the experimental and the theoretical standard deviation are very close one to another which means that the Poisson estimation is legit.

| $\bar{N}$ | $\sigma_{\bar{N}}$ | $\sigma_{\bar{N},th}$ |
|-----------|--------------------|-----------------------|
| 6.89      | 2.37               | 2.62                  |

In order to confirm this hypothesis, we will compare the experimental and theoretical (given by the Poisson law) frequencies for each number of detection.

| Counts | Exp. distribution | Th. distribution |
|--------|-------------------|------------------|
| 1      | 1                 | 2.2              |
| 2      | 4                 | 7.6              |
| 3      | 12                | 17.5             |
| 4      | 24                | 30.2             |
| 5      | 34                | 41.6             |
| 6      | 37                | 47.7             |
| 7      | 47                | 46.9             |
| 8      | 36                | 40.5             |
| 9      | 33                | 30.9             |
| 10     | 23                | 21.3             |
| 11     | 9                 | 13.3             |
| 12     | 2                 | 7.6              |
| 13     | 3                 | 4.0              |
| 14     | 0                 | 1.9              |
| 15     | 1                 | 0.9              |

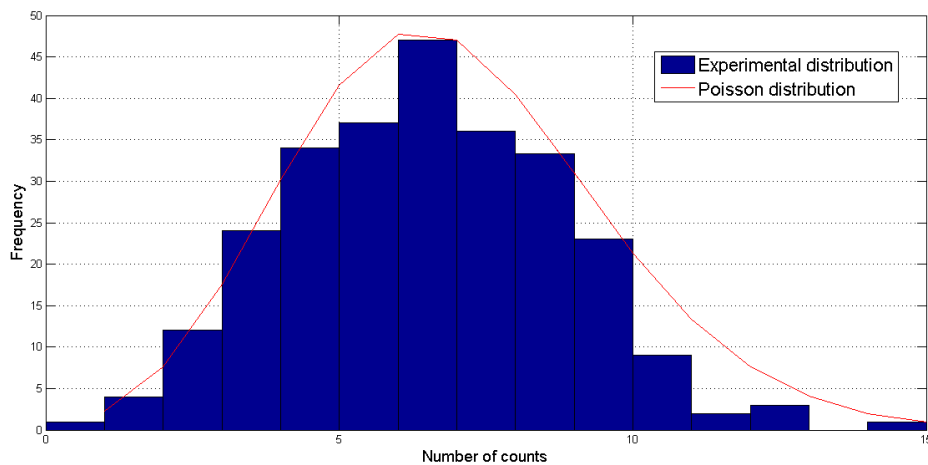


Figure 6: *Experimental and theoretical distribution*

At first sight, the two distributions seem to fit. To confirm (and in a more formal way), a  $\chi$ -square test will be done on our data.

| Counts         | Exp. distribution | Th. distribution | $\chi_i^2$ |
|----------------|-------------------|------------------|------------|
| 2 and under    | 5                 | 9.8              | 2.35       |
| 3              | 12                | 17.5             | 1.73       |
| 4              | 24                | 30.2             | 1.28       |
| 5              | 34                | 41.6             | 1.38       |
| 6              | 37                | 47.7             | 2.4        |
| 7              | 47                | 46.9             | 0.0002     |
| 8              | 36                | 40.5             | 0.5        |
| 9              | 33                | 30.9             | 0.1        |
| 10             | 23                | 21.3             | 0.25       |
| 11             | 9                 | 13.3             | 1.4        |
| 12 and greater | 6                 | 14.4             | 4.9        |
| $\chi_{exp}^2$ |                   |                  | 16.29      |



Since there are 11 classes and two algebraic constraints, the parameter  $\nu$  used for the chi-squared test is  $\nu = 9$ . With  $\alpha = 0.05$ , the tables give a value of  $\chi^2_{k=9, \alpha=5\%} = 16.92$ . As  $\chi_{exp} < \chi_{table}$ , we can affirm that the decay distribution follows a Poisson distribution with 95% confidence.

Finally it is interesting to see what would have happen by considering the whole experiment as one measurement which directly gives the mean value  $\bar{N} = 6.89$ , or as a longer experiment.

In the first case, the estimated error  $\epsilon_1$  is given by

$$\epsilon_1 = \frac{\sigma_{\bar{N}}}{\bar{N}} = \frac{N}{\sqrt{N}} \frac{1}{\sqrt{N}} = 0.381$$

In the second case, we calculate the error as follows

$$\epsilon_2 = \frac{\sigma_{\bar{N}}}{\bar{N}} = \frac{\sqrt{\sum_i N_i}}{\sum_i N_i} = \frac{1}{\sqrt{\sum_i N_i}} = 0.024$$

We obtain  $\epsilon_2 \ll \epsilon_1$  which seems logic because even if the two experiments have the same mean value, the deviation is weighted by the high amount of measurements in the second case. Thus, the result is more reliable.

### 2.5.2 High mean value

As the analysis does not differ from the last paragraph, we will not repeat it. We will simply note that the distribution tends to a Gaussian through a small effort of abstraction.

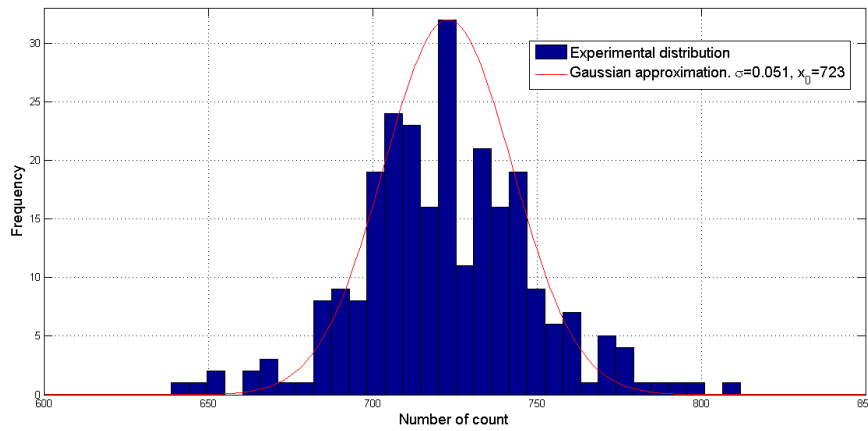


Figure 7: *Experimental results and gaussian approximation with  $\sigma = 0.051$  and  $x_0 = 723$*

### 3 Results and analysis

#### 3.1 Gamma spectrometry with scintillation and germanium detector

##### 3.1.1 Scintillation detector

First of all, we measure the spectrums of some different known sources. The spectrum is taken on computer trough the analyzer, so that the x-axis is not calibrated in energy but only on a 2048 channels range. We thus choose the more visible peak to define the x-axis values in energy. Here are some spectrums and some explanations about the origin of the different peaks.

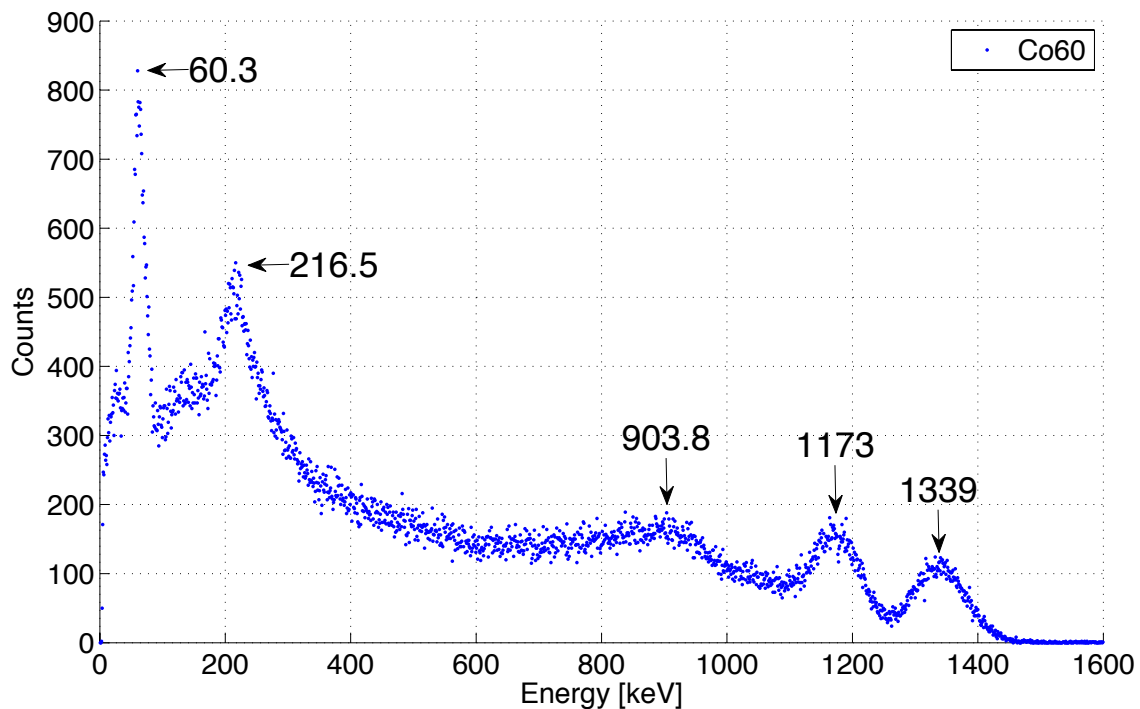


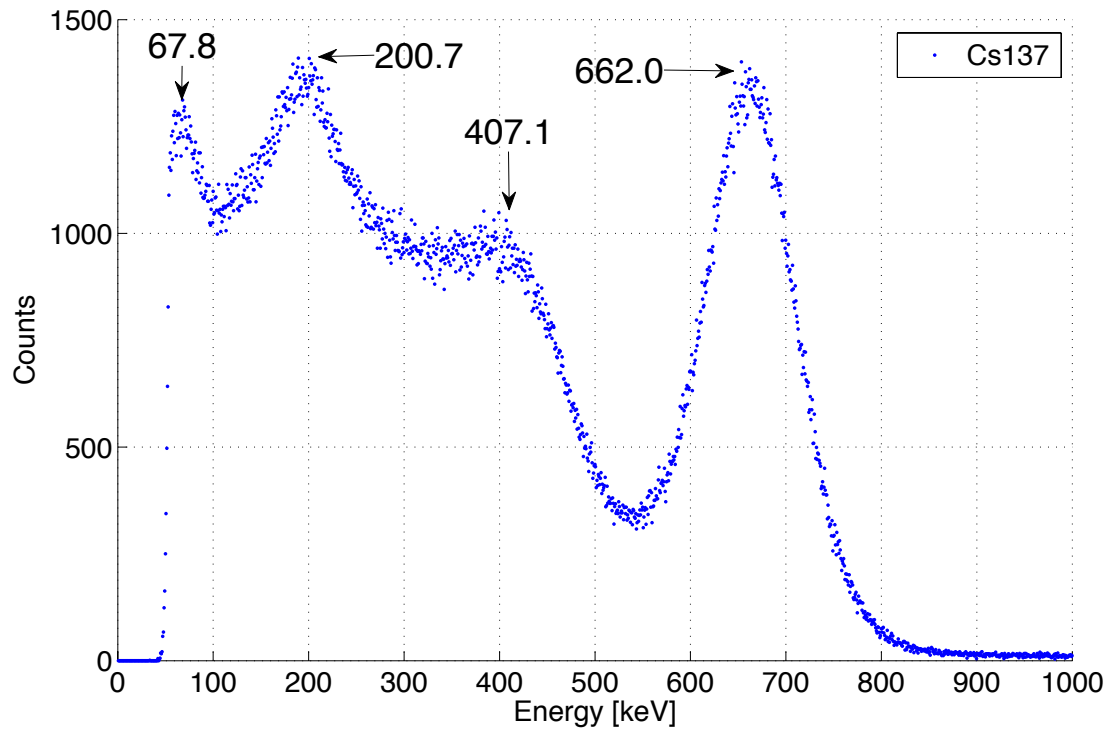
Figure 8: *Co60 spectrum*

In this first spectrum, Co60 decay was observed. We notice five distinct peaks. The first, around 60.3 keV corresponds to the X resulting of photoelectric effect on the lead collimation because it is the smallest in energy and we obtain an energy of 72.1 keV for an electronic transition between shell  $K$  to  $L_1$  for the lead, using equation (6).

Then we have a back scattering peak at 216.5 keV. This could be explained by the fact that equation (5) gives a maximum of 214.5 keV an expected  $E_\gamma = 1.332$  MeV. The peak at approximately 900 keV is due to the end of Compton effect. We can also calculate it theoretically using (3), 1117 keV.

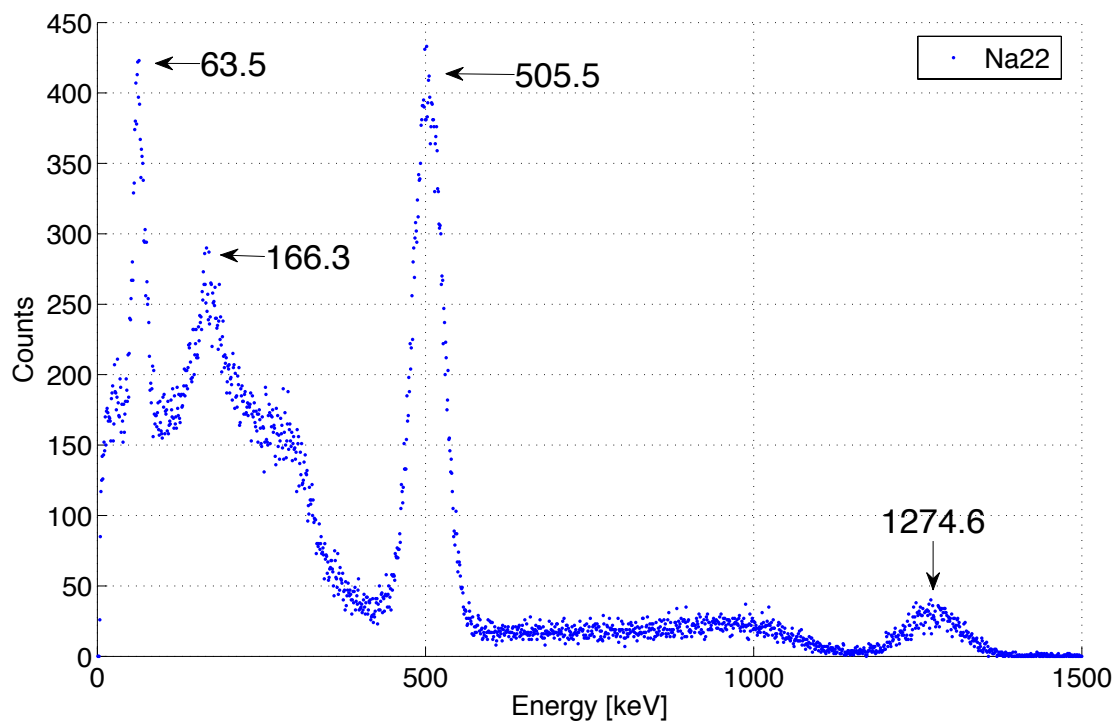
Finally the two last peaks are the  $\gamma$  radiations of the Co60 decay as we can see on the diagram in [1]. Here  $\gamma_1$  at 1.173 MeV (1.173 MeV in [1]) and  $\gamma_2$  at 1.339 MeV (1.332 MeV).

For the next spectrums, we just make a list of the peaks and their origins.

Figure 9: *Cs137* spectrum

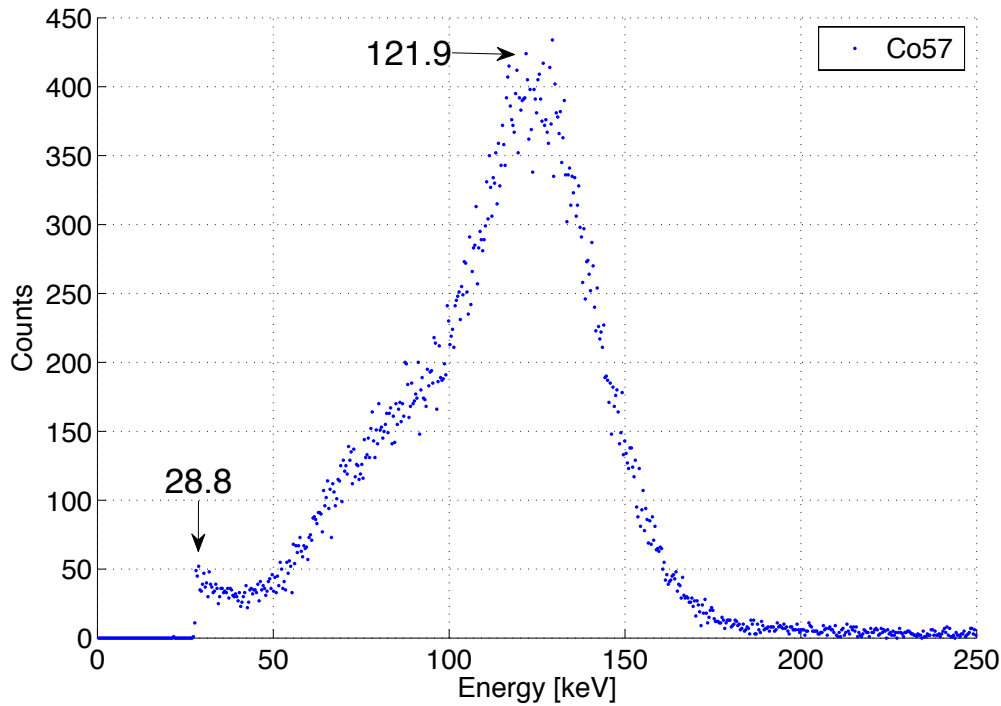
▷ 67.8 keV: lead collimation

▷ 200.7 keV: back scattering

▷ 0.662 keV:  $\gamma_1$ Figure 10: *Na22* spectrum

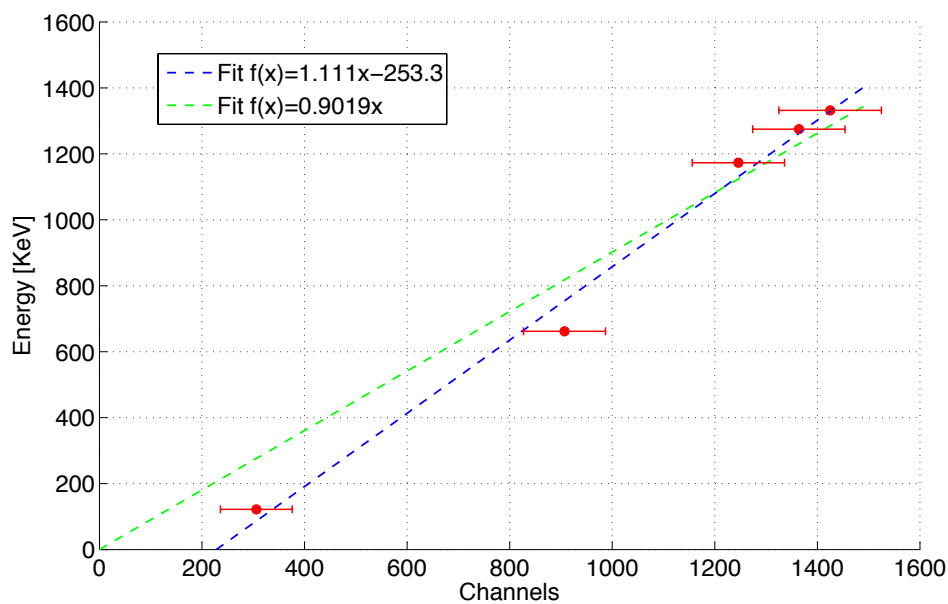
▷ 63.5 keV: lead collimation

▷ 166.3 keV: back scattering of  $\gamma_1$  and  $2\gamma$ ▷ 505.5 keV:  $2\gamma$  at 511 keV from electron-positron annihilation▷ 1.2746 MeV:  $\gamma_1$

Figure 11: *Co57 spectrum*

The spectrum of Co57 shows two visible peaks. Our expectations were on finding three peaks for  $\gamma_1$  14.4 keV,  $\gamma_2$  121.9 keV and  $\gamma_3$  136.3 keV. In our results, the  $\gamma_1$  is not visible and the 28.8 keV peak may corresponds to back scattering. Finally, the  $\gamma_2$  and  $\gamma_3$  peaks are mixed together in a big peak due to the weak resolution of the NaI detector which cannot distinguish peaks separated by only 15 keV.

In order to use the scintillator, we verify a linear relation between the energy given on the NaI crystal by radiations and the amplitude of pulses at the output of the detector and spectrometry chain. To do that, we used the different spectrums of known sources and we choose the more visible peaks to find the correspondance between energy and channels on the computer.

Figure 12: *Verification of linear spectroscopy chain*

The fits on the datas reveals a linear relation but is more precise with a additionnal parameter, maybe because of a constant noise in the chain or some errors.

Then, we would like to verify the dependence of the resolution  $\sigma_E/E$  in function of  $E$  for the photons detection. To do that, we fit the peaks of the photons in spectrums with gaussians. Then we obtain the standard deviations and the mean values which are  $\sigma_E$  and  $E$  respectively.

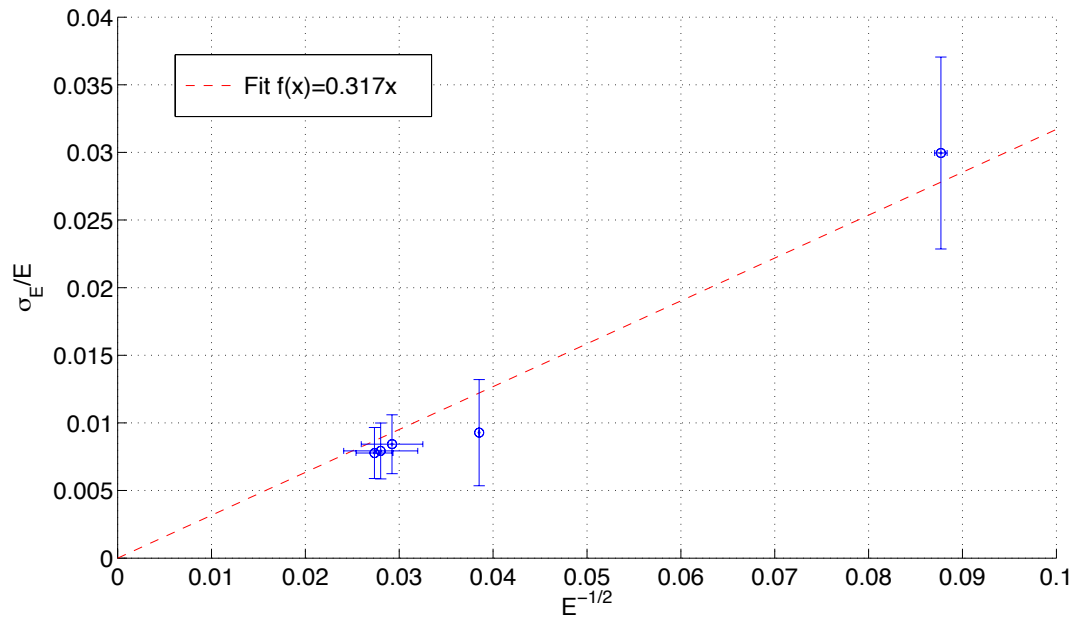


Figure 13: *Resolution of peaks depending on the energy*

The dependence of the resolution seems to be in function of  $E^{-1/2}$  as we can read it in the different notices. But we should have more peaks to be very sure of our results.

### 3.1.2 Germanium detector

We use in this point another detector which works with a different principle as explained in the theory. Firstly we have to calibrate it in measuring some spectrums of known energies. Here are two spectrums and the calibration relation.

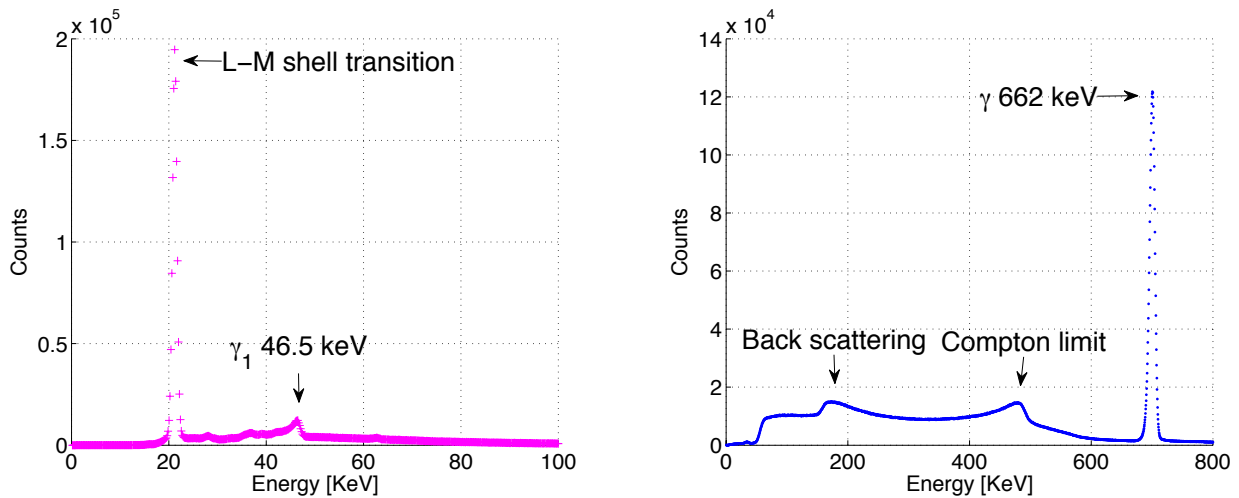


Figure 14: Spectrums of Pb210 and Cs137 with Ge detector

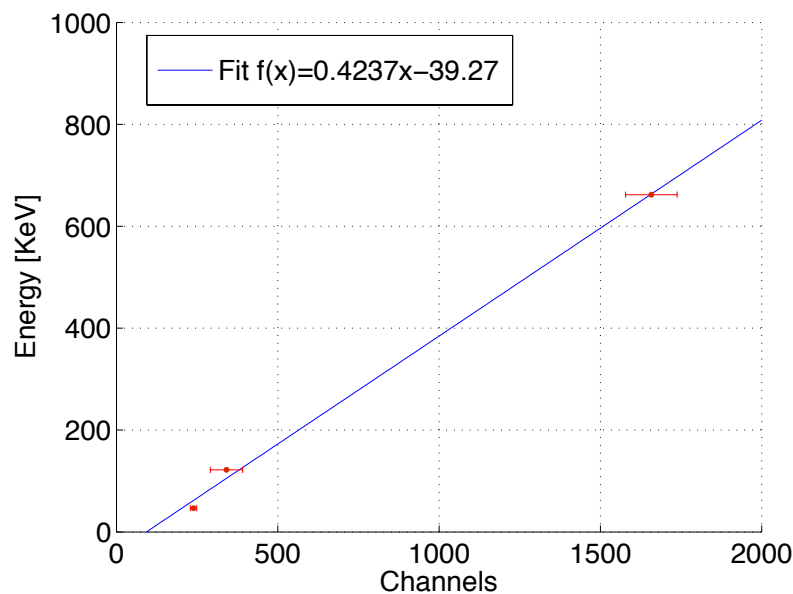
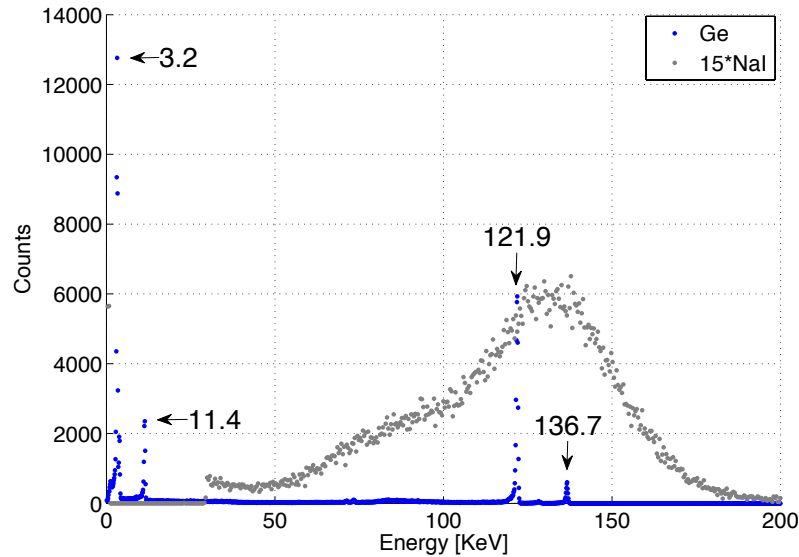


Figure 15: Calibration Ge detector

Then we compare the spectrums of Co57 obtained with both detectors.

We see clearly a difference between the two detectors. The semiconductor one gives precise peaks of energy and less noise. This comes from the functioning of the different detectors. Indeed, with the photomultiplier, an amplitude at the output can result from a wider range of energy detected on the scintillator because of the multiple photoelectric effects on the dynodes and so the output current. Thus the germanium detector shows distinctly the two  $\gamma_2$  and  $\gamma_3$  peaks of Co57, what we did not have with NaI detector. We also clearly see the  $\gamma_1$  at 11.4 keV (14.4 keV) peak that we did not have before. The 3.2 keV peak could correspond to  $K_\alpha$  radiation of iron (6.4 keV). By calculating the sum of the counts for each peak, we find a proportion of 20% for the  $\gamma_1$  that is approximately twice higher than the literature value.

Figure 16:  $^{57}\text{Co}$  spectrums with both detectors

### 3.2 Photons attenuation in matter

When a beam of photon collides with matter, there are some energy losses, which are due to the effects described in the theoretical section. To simplify, we will consider two cases. Either the photon goes through the matter without interaction, or it is stopped by the material and vanishes. The law describing this attenuation is the following, called radioactive decay law.

$$I = I_0 e^{-\mu_d \cdot d} = I_0 e^{-\mu(E_\gamma, Z) \cdot x} \quad (8)$$

where  $I$  and  $I_0$  are the intensity of the photon beam respectively at the measurement point and at the origin of the source,  $\mu_d = \mu/\rho$  is the massic attenuation coefficient,  $d = \rho \cdot x$  is the linear density of the shield, and finally  $x$  is the thickness of the shield.

By changing the thickness of the shield, and reporting the intensity of the transmitted beam, we get the following graph.

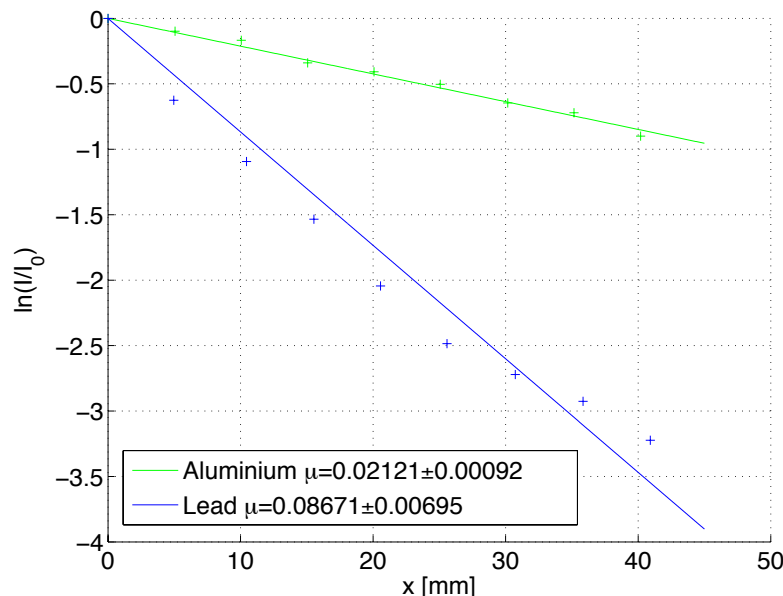


Figure 17: Determination of attenuation coefficient

In semilog scale, we first confirm that the law is exponential in  $x$ . A simple fit gives the experimental values for the (linear) attenuation coefficient for the Pb and the Al.

| Material | $\mu$ [ $cm^{-1}$ ] | $\mu_d$ [ $cm^2/g$ ] |
|----------|---------------------|----------------------|
| Pb       | 0.87                | 0.076                |
| Al       | 0.21                | 0.078                |

First of all, we remark that  $\mu_d$  seems to be constant. This fact has also been noticed in other experiments from our group, but has to be done on more materials in order to be correct. We also see that the lead is a way more efficient way to protect ourselves from radiations than the aluminium. This can be partially explained by the difference of density of these two elements. Since the lead is more dense than the aluminium, the photon is statistically more likely to interact with it, and lose its energy.

Secondly, if we refer to the tables D.6 and D.7 (general notice) which give the value of  $\mu$  depending on the energy, we get that these coefficients correspond to an energy of the incident photon beam of 0.8 MeV (Pb) and 0.62 MeV (Al). According to the decay scheme of  $^{137}\text{Co}$ , the photon beam has an energy of 0.662 MeV. Since these values are in the right order of magnitude, the experience fits with the theory.

### 3.3 Coincidences, estimation of Co57 activity

This section is about detecting coincidences between events coming from the same source in the two different detectors. The coincidences selector is a device that emits a signal each time it detects input signals at the same time, so if there is time superposition in the pulses at its input.

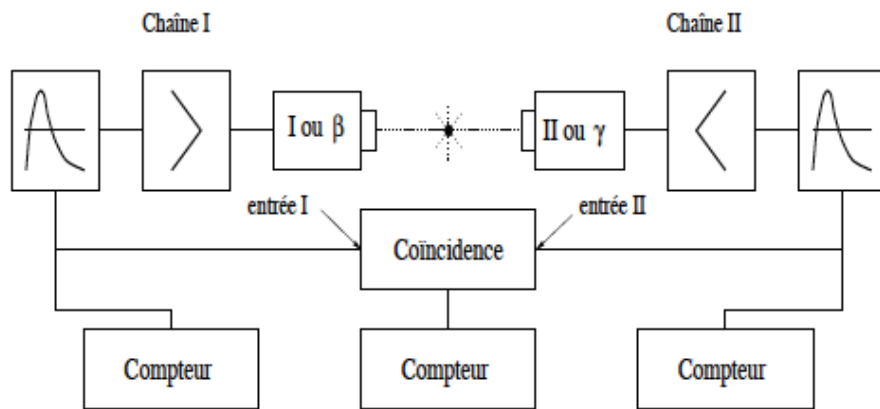


Figure 18: Setup to detect coincidences

We define the resolution time  $2\theta$  of the selector as the maximal time between two pulses of time  $\theta_1$  and  $\theta_2$  which are detected as a coincidence.

$$2\theta = \theta_1 + \theta_2 \quad (9)$$

We reference different kinds of coincidences. The true ones result from the detection in the two detectors of a particle coming from the same decay. We also have true coincidences that are the detections of the background noise as cosmic radiation. False coincidences are characteristics of detections in the two detectors at the same time that don't result from the same decay. Finally, we find parasite coincidences when a particle scatters from a detector to the other.



### 3.3.1 Determination of the resolution time

The measure of the selector's resolution time is made with two independent sources which is not correlated and emit in only one detector, what we ensure by putting a lead block between the two sources. So we find the rate of coincidences that appear when we are not supposed to have them. As we can see in [2], the mean rate (counts per second)  $m_m$  of detected coincidences is given by

$$m_m = 2\theta m_1 m_2 + m_c \quad (10)$$

where  $m_1$  and  $m_2$  are the rates for each detector and  $m_c$  is the rate of counts due to the background noise.

Thus, by plotting  $m_m$  in function of the product  $m_1 m_2$ , we can determine the resolution time. We used two Cs137 sources and just took the counts with a window on the gamma peak.

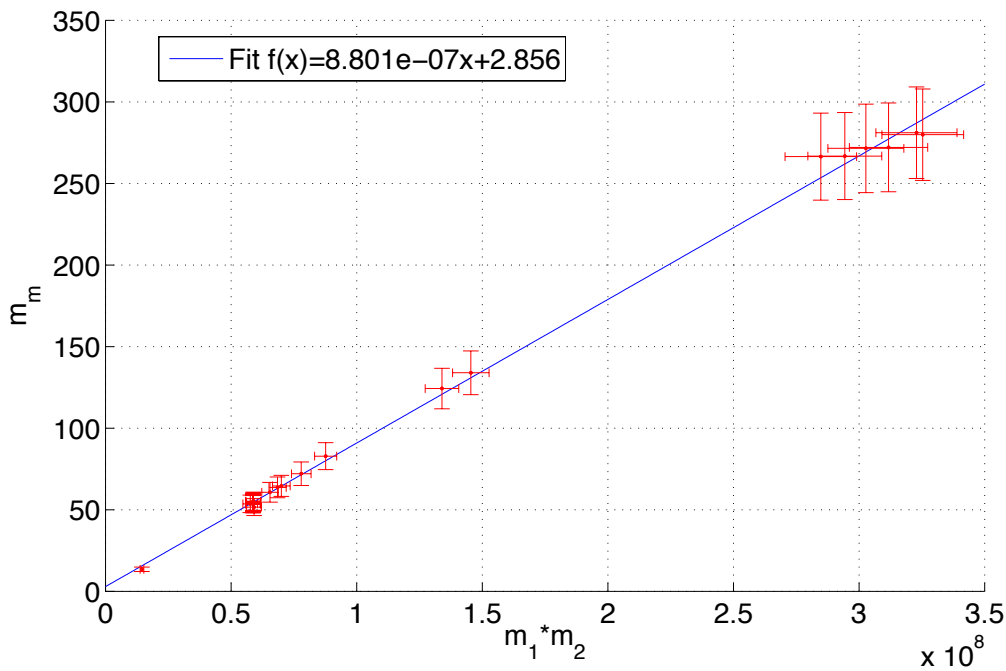


Figure 19: *Determination of resolution time*

We finally obtain:

$$2\theta = 880 \pm 15ns \quad (11)$$

### 3.3.2 Measurement of Co57 activity

Two gamma spectroscopy chains are used in coincidence with a Co57 source. The first with the germanium detector and the second with the NaI crystal, as previously. We put the window of the analyzer on the  $\gamma_1$  peak for the germanium detector and on the  $\gamma_2$  peak for the NaI detector. Even if the resolution of the scintillator is not good enough to capture the  $\gamma_2$  peak, we can take a narrow window and select the photons around 122 keV.

The activity, number of decay per second, is then given by

$$A = \frac{m_1 \cdot m_2}{2m_v} \quad (12)$$

with  $m_1$  the rate of counts in Ge detector,  $m_2$  in NaI detector and  $m_v = m_m - 2\theta m_1 m_2$  is the rate of detected coincidences corrected by the number of false coincidences with the resolution time found before.

| $m_1 [s^{-1}]$   | $m_2 [s^{-1}]$    | $m_m [s^{-1}]$      | $m_v [s^{-1}]$      | $A [MBq]$           |
|------------------|-------------------|---------------------|---------------------|---------------------|
| $42.50 \pm 0.51$ | $170.15 \pm 2.12$ | $0.0228 \pm 0.0005$ | $0.0164 \pm 0.0004$ | $0.2193 \pm 0.0107$ |
| $42.54 \pm 0.51$ | $173.38 \pm 2.17$ | $0.0250 \pm 0.0005$ | $0.0185 \pm 0.0005$ | $0.1995 \pm 0.0098$ |
| $42.46 \pm 0.51$ | $164.29 \pm 2.05$ | $0.0169 \pm 0.0004$ | $0.0108 \pm 0.0003$ | $0.3235 \pm 0.0159$ |
| $41.22 \pm 0.49$ | $161.42 \pm 2.02$ | $0.0200 \pm 0.0004$ | $0.0141 \pm 0.0003$ | $0.2352 \pm 0.0115$ |
| $39.51 \pm 0.47$ | $163.56 \pm 2.04$ | $0.0100 \pm 0.0002$ | $0.0043 \pm 0.0001$ | $0.7492 \pm 0.0367$ |
| $39.84 \pm 0.48$ | $160.67 \pm 2.01$ | $0.0140 \pm 0.0003$ | $0.0083 \pm 0.0002$ | $0.3825 \pm 0.0187$ |

Table 1: Table of measurements, rates and activity, Co57 source

We finally obtain by taking the mean value of results:

$$A = 0.352 \pm 0.017 \text{ MBq} \quad (13)$$

which is in the same order of magnitude than the referenced activity of this source which was 0.37 MBq (in 2012).

### 3.4 Period measurements of Fe57 14.4 keV level

Now, let us determine the period or half life of the 14.4 keV level for Fe57 which is obtained by the Co57 decay, as shown on the decay diagram below. As before, the semiconductor detector is focused on the  $\gamma_1$  peak of the Co57 source and the NaI one on the  $\gamma_2$ . Coincidences must be obtained between the detectors if the lines  $\gamma_1$  and  $\gamma_2$  are in cascade.

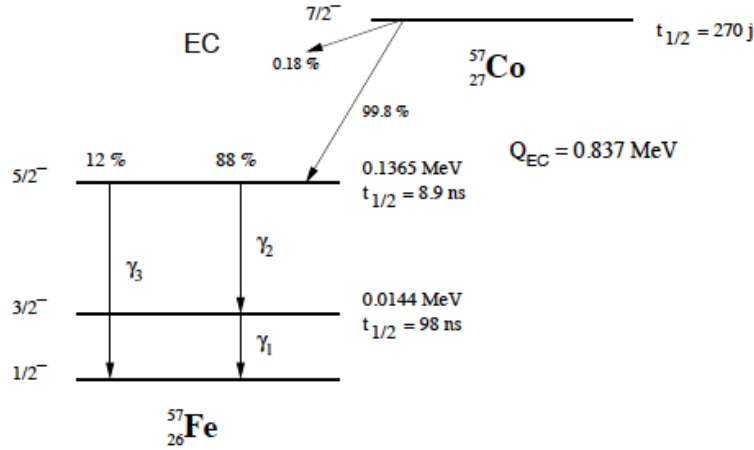


Figure 20: Decay diagram Co57

We define the time  $t_{12}$  as the interval of time detected between the  $\gamma_2$  and  $\gamma_1$  emissions. The time intervals are measured with a time-amplitude converter (CTA) which gives a pulse proportionnal to the time interval between two input pulses (here the pulses of the gammas detections).

The distribution of the time intervals  $t_{12}$  is given by

$$p(t_{12}) = a \cdot e^{-\frac{t_{12}}{\tau}} \quad (14)$$

with  $\tau$  is the half life time of the level, the 14.4 keV level in this case.

The experimental setup allows us to measure the experimental distribution  $p(t_{12})$  (or proportionnal signal) in function of the channels of the analyzer. In fact, this curve is a superposition of a gaussian due to the resolution time of the devices and an exponential decreasing coming from the distribution wanted as explained in [2].

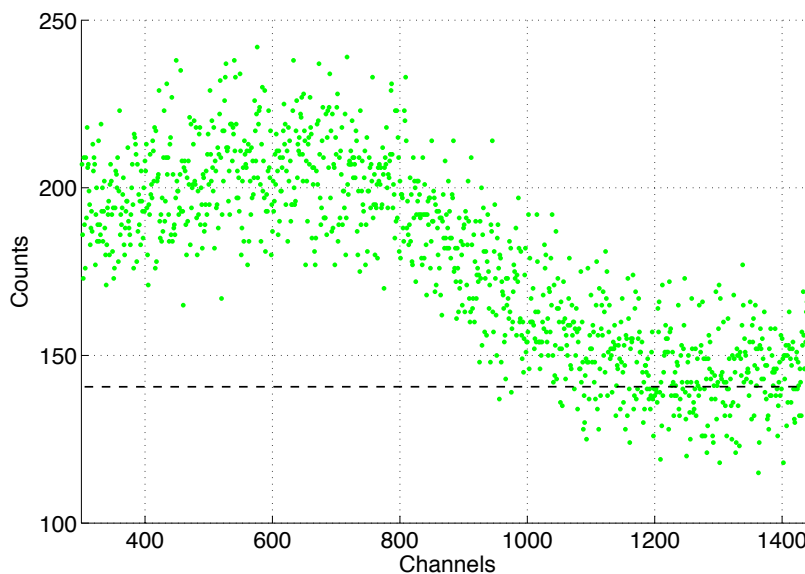


Figure 21: Results for CTA measurements, Co57

We interest us on the exponential decreasing between channels 600 and 1000 and would like to fit the curve in comparison with the distribution  $p(t_{12})$ . We also cancel the background noise value that is around 140 counts before the fit. First we determine the calibration relation to have the time equivalent to the channel's number.

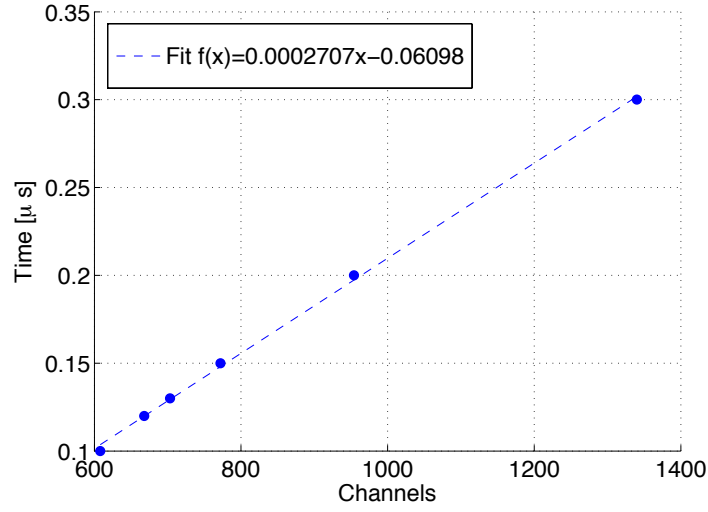


Figure 22: Calibration curve and relation for CTA

Then here are the results of the fit in time units:

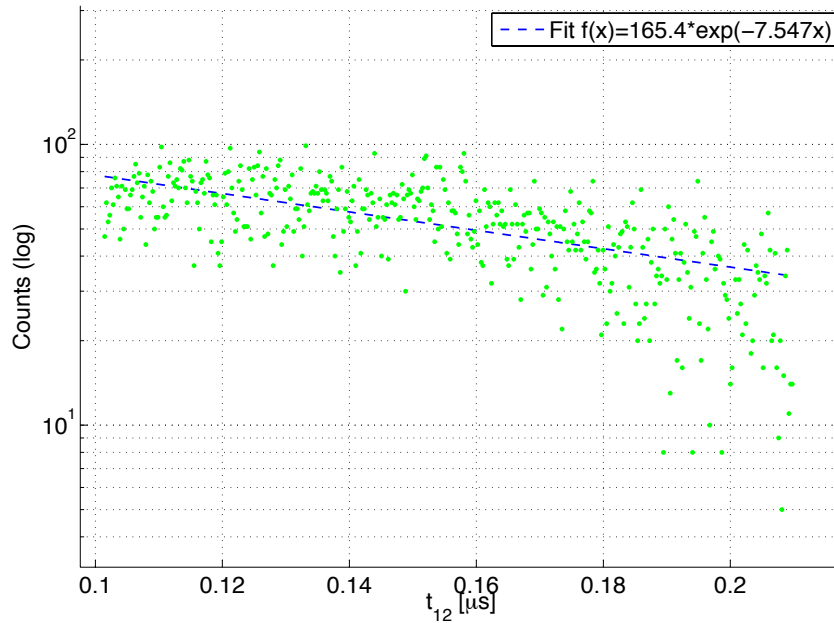


Figure 23: Curve fitting for exponential decreasing

Thus the experimental value of  $\tau^{-1}$  is  $7.547 \pm 0.907 \mu s^{-1}$ . So that the period (half time of life) of the 14.4 keV level is

$$t_{1/2} = \tau \cdot \ln(2) = (0.1325 \pm 0.0159) \cdot \ln(2) = 0.0918 \pm 0.0110 \mu s = 91.8 \pm 11.0 ns \quad (15)$$

According to the decay diagram, this period should be equal to 98 ns, what makes our results in the right order of magnitude. Note that the calibration and the curve fitting are crucial in this point and the way we took is not precise enough to determine the period of the level with good confidence.

## 4 Conclusion

This set of experiments were a small introduction to nuclear physics. We first determined that the nature of nuclear phenomena follow a Poisson law. We then showed the spectrum of different elements, using a germanium and a scintillation detector. We also measured the attenuation coefficient of two different type of shields. We finally used the principle of coincidence to measure the activity of Co57. Both of our results gave satisfying values, according to the existing theory.

## References

- [1] *Notice générale des Travaux Pratiques de Physique Nucléaire*, Dr Silvia Tentindo Ansermet, LPHE, EPFL, September 2008
- [2] *Travaux pratiques de physique nucléaire, Expérience X, Désintégration du Cobalt 57, détecteur au germanium*, LPHE, EPFL, September 2012
- [3] *Introduction à la physique nucléaire et corpusculaire*, Prof. Olivier Schneider, LPHE, EPFL, October 2003